

## **Daily and long-term variations of the effective temperature history and their correlation with those of stay cable force**

\*Chien-Chou Chen<sup>1)</sup>, Wen-Hwa Wu<sup>2)</sup> and Chun-Yan Liu<sup>3)</sup>

<sup>1), 2), 3)</sup> *Department of Construction Engineering, NYUST, Yunlin 640, Taiwan*

<sup>1)</sup> [ccchen@yuntech.edu.tw](mailto:ccchen@yuntech.edu.tw)

### **ABSTRACT**

Various studies have indicated that the monitoring of cable force may be the most efficient approach to diagnose the damages of cable-stayed bridges if it is feasible to accurately recognize and then filter out the environmental temperature effect. A recent study by the authors discovered that an effective temperature defined by combining all the contributions from stay cable, bridge girder, and pylon is most strongly correlated with the cable force. Based on the above study, this work further applies the ensemble empirical mode decomposition to process the time histories of cable force and effective temperature for an extradosed bridge located in central Taiwan. It is evidently observed that the cable force and effective temperature can both be categorized into daily variation, season variation, and high-frequency noise with the order of decreasing weight. Moreover, a time shift around 1 to 2 hours generally exists between the daily variations of both investigated quantities. The correlation analysis performed for the one-year data revealed that daily and season variations have to be distinguished for accurately assessing the temperature effect on the variation of cable force.

### **1. INTRODUCTION**

In order to efficiently manage the safety and serviceability of bridges, numerous methods with different strategies have been developed to evaluate the structural condition of bridges. Although visual inspection or experimental methods were often adopted for damage identification of long-span bridges, their applications are generally restricted to the accessible and pre-known local portion of structure with high damage potential. Recently, more studies have attempted to develop global damage detection methods and several of them revealed that structural health monitoring (SHM) is one of the feasible solutions to assess the structural condition of bridges. Although the techniques of structural health monitoring are frequently adopted for attempting to diagnose the possible damages of bridges, their feasibility and accuracy in practical applications remain to be extensively verified.

For cable-stayed bridges, it is apparent that the most critical structural component is the stay cable system because it suspends most of girder weight and is the primary

---

<sup>1)</sup> Associate Professor

<sup>2)</sup> Professor

<sup>3)</sup> Graduate Student

path for transmitting the live loadings on girder. Numerous studies have clearly demonstrated that the abnormal change in structural condition for a cable-stayed bridge would subsequently induce the force redistribution of its cable system. Accordingly, the monitoring of cable force is regarded as a royal road to diagnose the possible damages of cable-stayed bridges. The feasibility of this approach, however, deeply depends on accurate identification and filtration of the environmental temperature effect because it can also significantly alter the cable force in practical applications (Chen 2010). Exploiting the convenient determination of cable force using the identified modal frequencies from ambient vibration measurements, a recent study by the authors attempted to explore this problem by performing a long-term monitoring on the cable forces and temperatures in various structural components of Ai-Lan Bridge, an extradosed bridge located in central Taiwan (Chen 2012). It was discovered that an effective temperature defined by combining all the contributions from stay cable, bridge girder, and pylon with appropriate consideration of their geometrical setup is most strongly correlated with the cable force.

Based on the above study, the current work further applies the empirical mode decomposition (EMD) to process the time histories of cable force and effective temperature for a more detailed investigation of their correspondence. The intrinsic mode functions (IMF) resulted from performing EMD on both time histories with the same duration of approximately one month are closely examined for each of the four seasons. Such elaborate procedures are aimed to more effectively categorize different components of both the cable force and the effective temperature for further denoising and more specific correlation analyses. With these decomposed IMF's, the correlation coefficients between the effective temperature and the cable force are computed in this study for various possible combinations in order to find the best correlated components of these two quantities.

## **2. INITIAL ANALYSIS OF CABLE FORCES AND EFFECTIVE TEMPERATURES**

The studied object, Ai-Lan Bridge, is a three-span symmetric concrete extradosed bridge with a main span of 120m. The cable system is arranged in a harp shape along the centerline of girder with nine pairs of stay cables on each side of every pylon. The bridge commenced its construction in 2004 and was opened for traffic in 2008. A monitoring system was established during its construction stage. The function of the monitoring system is to measure the stress and/or strain conditions of critical bridge components as well as the temperature variations of surrounding air and various structural components. In addition to the existing monitoring system, a simple device composed of a fiber Bragg grating (FBG) sensor attached on a fishing line (Chen 2008) was developed by this research group to adequately measure the ambient vibration signals of the cable system. These FBG sensors are installed on Cables E01 to E18, all the 9 pairs of cables on one side of a pylon. From those signals, the natural frequencies of each cable are identified and then employed to determine the corresponding cable forces with the ambient vibration method. As for the temperature measurements, a number of thermocouples were installed at six cross sections of girder and two cross sections of pylon in the original monitoring system to measure the structural temperature. Moreover, several thermometers were also deployed outside and inside

three selected cross sections of girder to record the air temperature. Nonetheless, no temperature sensors were aimed at taking the cable temperature in the original monitoring system. To fit this cavity, a cable specimen of 1 m long was also made by this research group for imitating the real cable by assembling the same number of tendons inside an HDPE tube (Chen 2012). FBG temperature sensors were attached on the surface of certain inside tendons to intimately take the temperature of the cable specimen placed on the bridge deck.

Several important conclusions have been made in the recent study by the authors (Chen 2012) regarding the measurements and analyses of temperatures and cable forces for Ai-Lan Bridge. Fig. 1 depicts a typical example illustrating the daily temperature variations of air and various structural components. It is apparently observed from this figure that the daily temperature variations at different locations share a similar fluctuation curve mainly composing of a steeper increasing trend during the daytime and the other slower decreasing trend during the nighttime. However, closer examination reveals two major distinctions in variation magnitudes and time lags among these different temperature measurements. As far as the daily variation magnitude is concerned, the air temperature exhibits a much larger value than those for the cable, the girder and the pylon in a decreasing order. On the other hand, the temperatures of various structural components all demonstrate time lags in the daytime rising curve with respect to the corresponding air temperature. More specifically, the significance of this time lag in temperature follows the order of girder, cable, and pylon. It should be noted that the above trends are consistently held all year round from inspecting the data covering one year. The exceptions only occur in the days under cold fronts to considerably reduce the variation magnitude and spoil the daytime increasing trend.

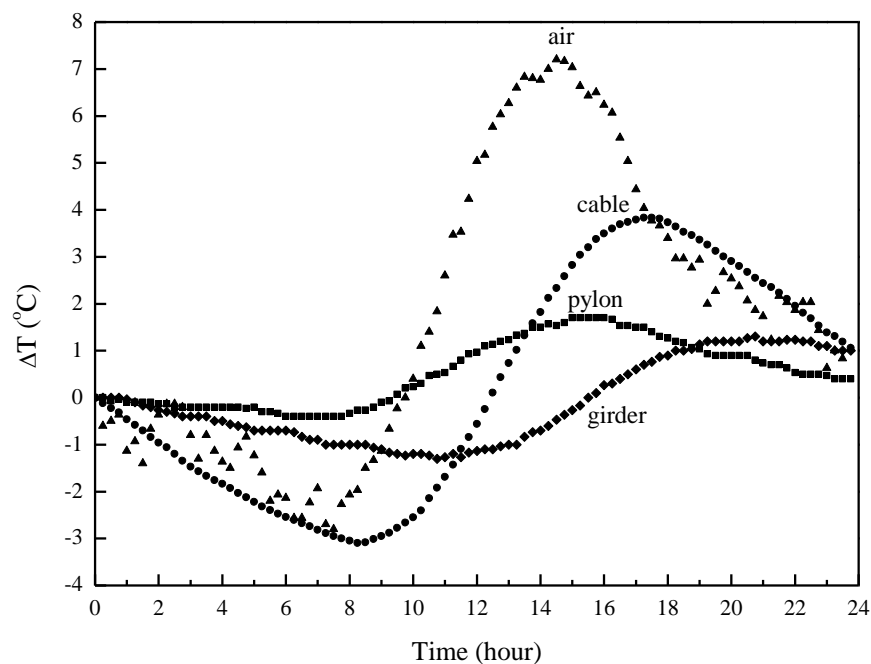


Fig. 1 Daily temperature variations of air and various structural components

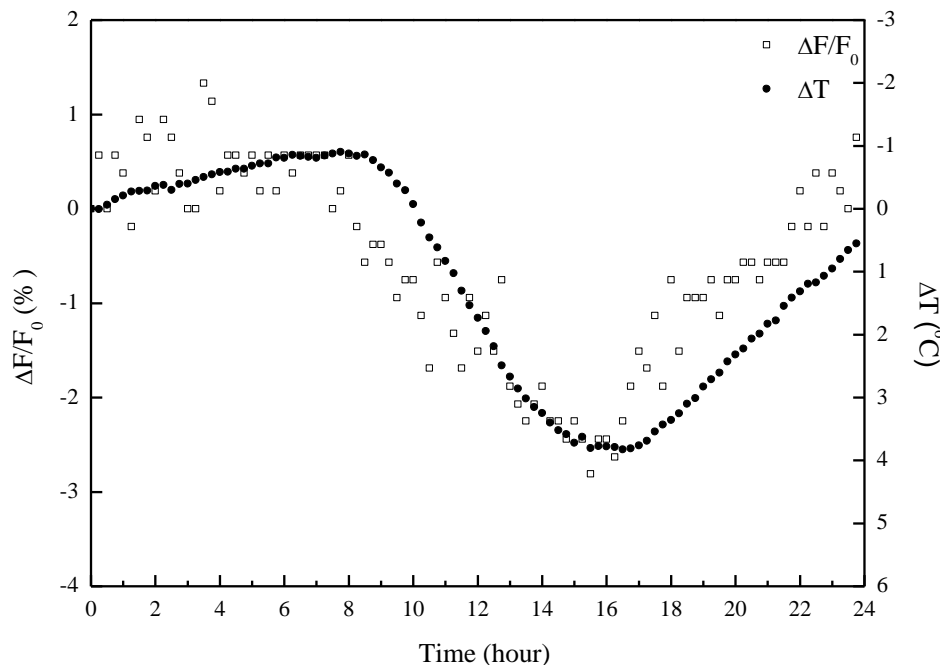


Fig. 2 Daily variations of cable force and effective temperature

To obtain the data of cable force, the ambient vibration signal from the FBG sensor installed on each cable was automatically collected for 300 sec every 15 minutes. The measured displacement time history of cable vibration is first transformed into the frequency domain by the discrete Fourier transform (DFT) technique. Then, the cable frequencies can be clearly identified without ambiguity from the corresponding Fourier amplitude spectrum. In other words, there are totally 96 identified frequency values for each cable per day. Based on the string theory, the internal force  $F_0$  of a stay cable at a reference time  $t_0$  can be expressed in terms of its modal frequency as

$$F_0 = 4\bar{m}L^2 \left( \frac{f_{n0}}{n} \right)^2 \text{ or } \varepsilon_0 = \frac{F_0}{EA} = \frac{4\bar{m}L^2}{EA} \left( \frac{f_{n0}}{n} \right)^2 \quad (1)$$

where  $L$ ,  $\bar{m}$ ,  $E$ , and  $A$  represents the length, mass per unit length, Young's modulus, and cross-sectional area of cable, respectively,  $f_{n0}$  signifies the natural frequency of the  $n$ -th mode in Hz, and  $\varepsilon_0$  symbolizes the axial strain, both at that reference time. It can also be noted from Eq. (1) that the cable force is proportional to the square of the cable frequency. Considering the corresponding quantities  $F_1$ ,  $f_{n1}$ , and  $\varepsilon_1$  at any other time instant  $t_1$ , subtraction of the two sets of quantities at different time instants directly leads to

$$\frac{\Delta F}{F_0} = \frac{F_1 - F_0}{F_0} = \frac{f_{n1}^2 - f_{n0}^2}{f_{n0}^2} = \frac{\Delta f_n^2}{f_{n0}^2} = \frac{\varepsilon_1 - \varepsilon_0}{\varepsilon_0} = \frac{\Delta \varepsilon}{\varepsilon_0} \quad (2)$$

It is well known that the change of structural temperature can directly induce the variations in internal stress and strain of a structural system. To more systematically analyze the temperature effect on the variation of cable force, a couple of simplifications by neglecting the thermal gradient and the secondary effect due to structural constraints were assumed. Under such circumstances, a stay cable with an inclination angle  $\theta$  would be subjected to a variation of strain

$$\begin{aligned}\Delta\varepsilon = \varepsilon_1 - \varepsilon_0 &= \alpha_G \Delta T_G \cos^2 \theta + \alpha_p \Delta T_p \sin^2 \theta - \alpha_c \Delta T_C \\ &\approx -\alpha (\Delta T_C - \Delta T_G \cos^2 \theta - \Delta T_p \sin^2 \theta) = -\alpha \Delta T_{eff}\end{aligned}\quad (3)$$

if the temperature variations of pylon, girder, and cable are  $\Delta T_p$ ,  $\Delta T_G$ , and  $\Delta T_C$ , respectively, between the time instants  $t_0$  and  $t_1$ . It should be noted that  $\alpha_p$ ,  $\alpha_G$ , and  $\alpha_c$  in Eq. (3) represent the thermal expansion coefficients of pylon, girder, and cable, respectively. For practical cases where the pylon and girder are commonly made of concrete and the steel cables are typically adopted, these thermal expansion coefficients can be approximated with the same value  $\alpha$ . Substitution of Eq. (3) into Eq. (2) then gives

$$\frac{\Delta F}{F_0} = \frac{\Delta f_n^2}{f_{n0}^2} \approx -\frac{\alpha}{\varepsilon_0} (\Delta T_C - \Delta T_G \cos^2 \theta + \Delta T_p \sin^2 \theta) = -\frac{\alpha}{\varepsilon_0} \Delta T_{eff}\quad (4)$$

According to Eq. (4), it is obvious that the square of the cable frequency variation (and consequently the cable force variation) normalized to its reference value should be proportional to the effective temperature variation  $\Delta T_{eff}$  combining the temperature effects from the pylon, girder, and cable. To investigate the effectiveness of the above analysis,  $\Delta f_n^2 / f_{n0}^2$  to indicate  $\Delta F / F_0$  is plotted in Fig. 2 together with the effective temperature variation for Cable E13 as an example. It should be noted that the ordinates for  $\Delta F / F_0$  and  $\Delta T_{eff}$  are defined in opposite directions for an easy comparison due to their negative correlation as shown in Eq. (4). Since the stay cables of Ai-Lan Bridge are all with an identical inclination angle of  $\theta = 17^\circ$  ( $\sin^2 \theta = 0.09$  and  $\cos^2 \theta = 0.91$ ), the contribution to the effective temperature variation from the temperature variation of pylon is trivial and can be neglected. From Fig. 2, it is evident that  $\Delta F / F_0$  follows a consistent trend with  $\Delta T_{eff}$ . Consequently, it can be verified that this simplified analysis is effective and the temperature is the major environmental factor for the variation of cable force without the occurrence of damages.

### 3. DECOMPOSITION OF EFFECTIVE TEMPERATURE AND CABLE FORCE

Although the results in Fig. 2 demonstrates a strong negative correlation between the cable force and the effective temperature for a duration of one day, the long-term effect of the effective temperature on the cable force requires further exploration. Because of several technical problems ever encountered in the initial year of the

installed FBG system, there are totally 223 days of effective signals intermittently collected from September of 2010 to August of 2011. Fortunately, approximately one month of continuous data can still be extracted for each of the four seasons. To more systematically investigate their correspondence, the empirical mode decomposition is first adopted in this study to process the time histories of cable force and effective temperature.

EMD is an adaptive method to decompose a signal into several intrinsic mode functions with balanced oscillations with respect to their zero means (Huang 1998). The procedure of EMD usually starts with constructing the upper and lower envelopes of the original signal by performing cubic spline interpolations to fit the local maxima and minima, respectively. The average of both envelopes can then be taken to determine a temporary baseline, which is subtracted from the original signal to complete the first round of sifting process. By repeatedly conducting such a sifting process until the number of zero crossings is very close to that of extrema, an IMF can eventually be obtained. Subsequently, subtraction of the extracted IMF from the original signal is carried out to yield the remained signal ready for decomposing the next IMF by similar sifting procedures. This process is reiterated until a monotonic signal, usually referred as the residue, is remained. Overall, the empirical mode decomposition of a signal can be mathematically expressed as:

$$y(t) = \sum_{k=1}^m c_k(t) + r(t) \quad (5)$$

where  $y(t)$  is the original signal,  $c_k(t)$  is the  $k$ -th IMF,  $r(t)$  is the residue, and  $m$  denotes the total number of obtained IMF's. It should be emphasized that the IMF's coming from the EMD process earlier usually have the content in a higher frequency range. Furthermore, a narrow-banded frequency content may not be guaranteed for each IMF due to the adaptive nature of this method.

Taking the one-month data of Cable E13 measured in the winter for example, the IMF's obtained from the EMD process for the variation of cable force and that of effective temperature are shown Figs. 3 and 4. It is clear that the first two IMF's of effective temperature force are composed of extremely high-frequency components, which are not possible to be present in temperature variation and should be considered as measurement noises. Therefore, these two IMF's are excluded from the temperature history in the subsequent correlation analysis for identifying all the IMF's of cable force closely related to the temperature variation. All the possible combinations of cable-force IMF's are checked to examine their correlation with the noise-free temperature. It is found that the highest correlation coefficient of  $-0.77$  can be obtained by combining IMF 5 of cable force up to the residue. This result indicates that the cable force components from IMF 5 to the residue are most related to the effect of temperature variation and the first four IMF's should also come from measurement noises.

Based on the above analysis, the denoised history of effective temperature by combining IMF 3 up to the residue and that of cable fore by incorporating IMF 5 up to the residue are displayed in Fig. 5. Careful examination on the local maxima and minima of these two time histories in this figure evidently discloses that the local

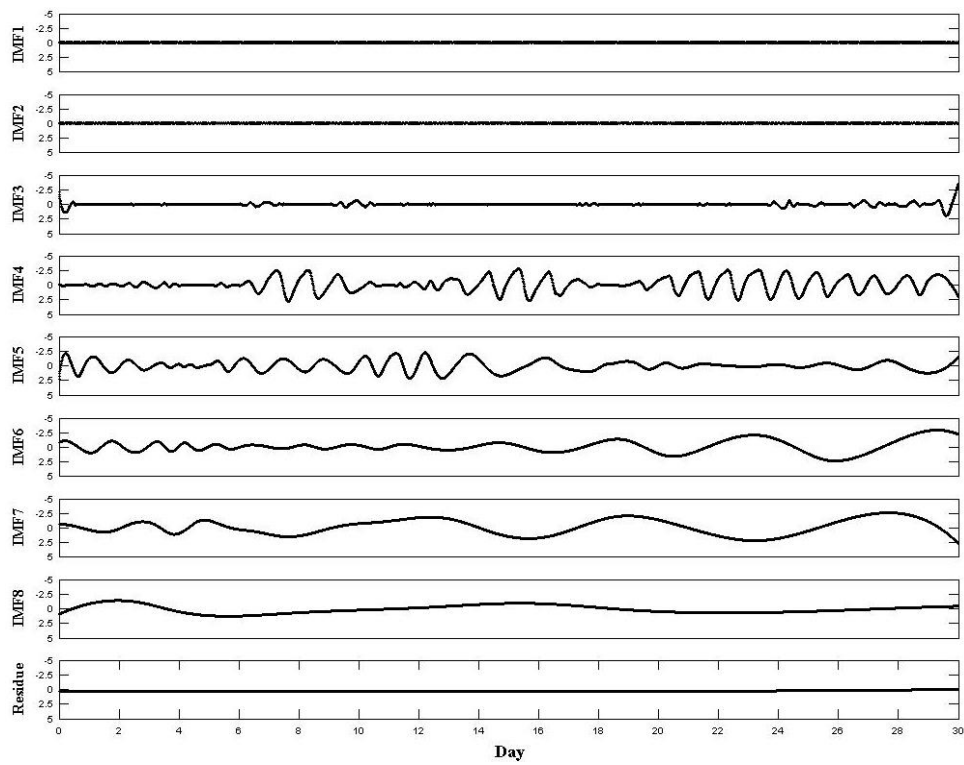


Fig. 3 IMF's of the effective temperature from EMD

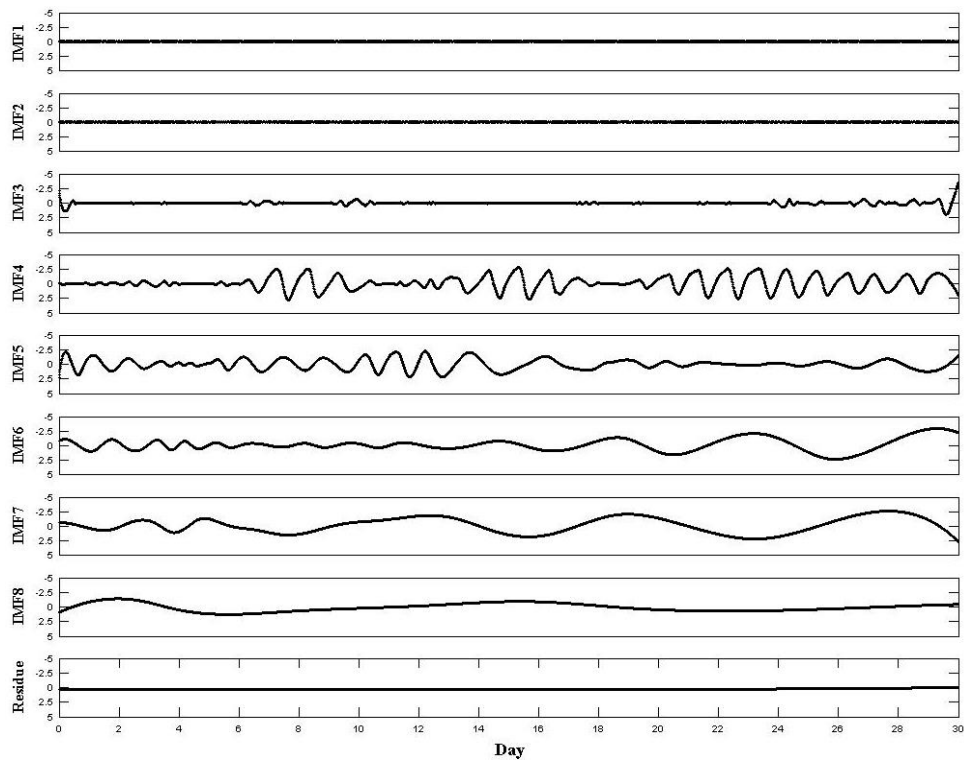


Fig. 4 IMF's of the cable force from EMD

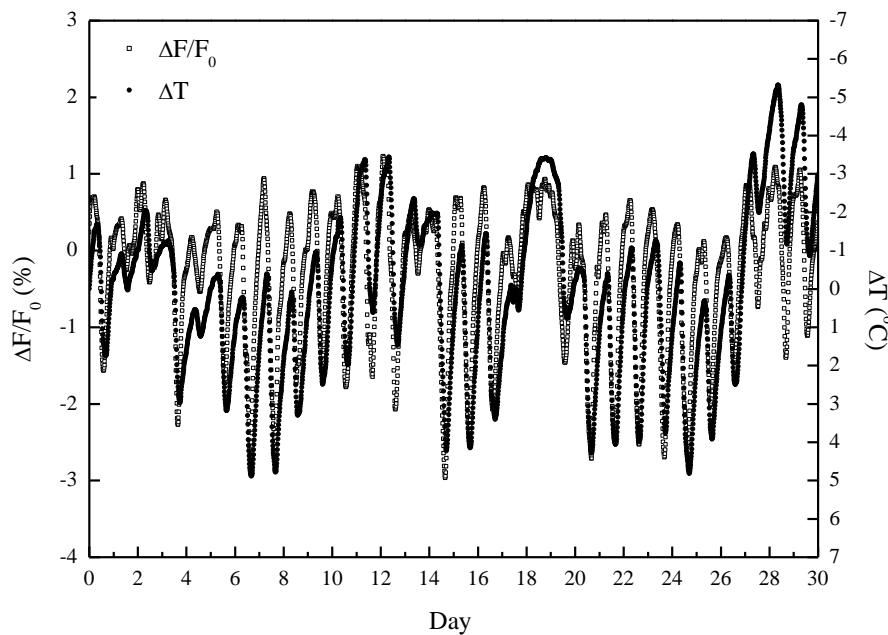


Fig. 5 Time histories of denoised effective temperature and cable force

extrema of both quantities do not occur simultaneously. In other words, there exists a clear time shift between these two quantities. Comparison of all the IMF's illustrated in Figs. 3 and 4 reveals that IMF 4 of the effective temperature and IMF 6 of the cable force are the most dominant components for both quantities, respectively, and demonstrate similar oscillations. An optimal time shift of 105 minutes (7 time increments of 15 minutes) can then be determined to attain the maximum correlation coefficient between these two IMF's. With this time shift applied, the correlation coefficient between the denoised histories of effective temperature and cable force is found to improve from  $-0.77$  to  $-0.85$ . Even so, enhancement can still be anticipated to further increase the corresponding correlation coefficient since Figs. 3 and 4 also show that the other minor IMF's of cable force do not correspond well with those of effective temperature, not to mention the feasibility of obtaining appropriate time shifts. In fact, it is not difficult to accept that the temperature variation in a whole year should be at least distinguished into the daily variation and the season (long-term) variation. Accordingly, the correlation would no doubt be raised if it is able to distinctively classify the temperature effect on the cable force variation into daily and season bases. Fig. 3 and 4, however, exhibit another crucial problem that a wide range of frequency components may be mixed together in an IMF resulted from the EMD process. To tackle this difficulty and then provide a better basis for discriminating the temperature effect on the cable force variation, the technique of ensemble empirical mode decomposition (EEMD) recently developed (Wu 2009) is further employed in this study.

Modified from EMD, EEMD is a noise-assisted data analysis method to ensure a narrow-banded frequency content for each IMF. The procedure of EEMD starts with adding a white noise with a zero mean and a standard deviation of certain level to the targeted signal. The noise-added signal is then decomposed into several IMF's with the

conventional EMD process. Such an operation is repeatedly conducted with different random white noises to produce numerous sets of IMF's. Finally, the average of all the corresponded IMF's in different sets is taken to determine the final version of each specific IMF. It is noteworthy that the purpose of adding a white noise to the original signal is to help create a uniform distribution in the frequency domain for generating well separated and narrow-banded IMF's. Although the individual EMD processes may yield the IMF's highly polluted by the added noises, all the artificial noises would be eventually cancelled out in the final averaging operation as long as the ensemble number is sufficiently large. It is no doubt that the EEMD process is much more time-consuming than the conventional EMD process and its computation cost increases with the ensemble number. To minimize such a disadvantage, the adoption of paired white noises with opposite values at each instant is proposed in the current study. With this setup, the perfect cancellation of noises can still be guaranteed all along the time history even if a significantly reduced ensemble number is taken.

For the same one-month data in the winter, the goal of creating well separated and narrow-banded IMF's can be easily achieved simply with 50 pairs of random white noises. Another important parameter to be determined in the EEMD process is the level of standard deviation for the added white noises. This noise level needs to be comparable with the amplitude of the original signal such that the addition of noise can induce the expected effect. For the time histories of effective temperature and cable force previously discussed, it is found that the noise level selected at 150% of the standard deviation of the original signal would consistently produce 11 stable IMF's together with the residue from the EEMD process. IMF 5 up to the residue of effective

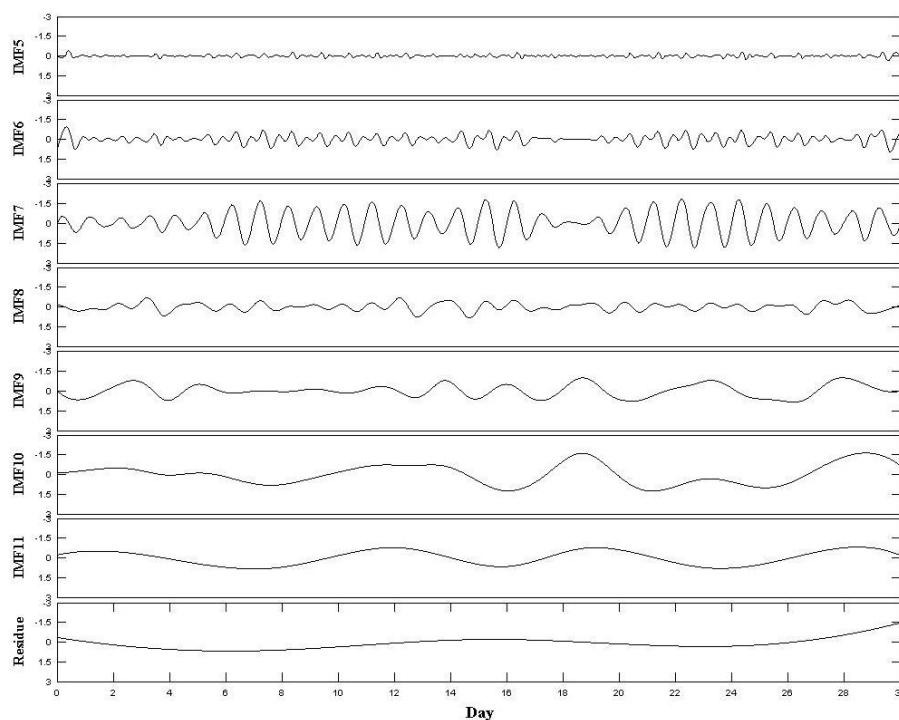


Fig. 6 IMF's of the effective temperature from EEMD

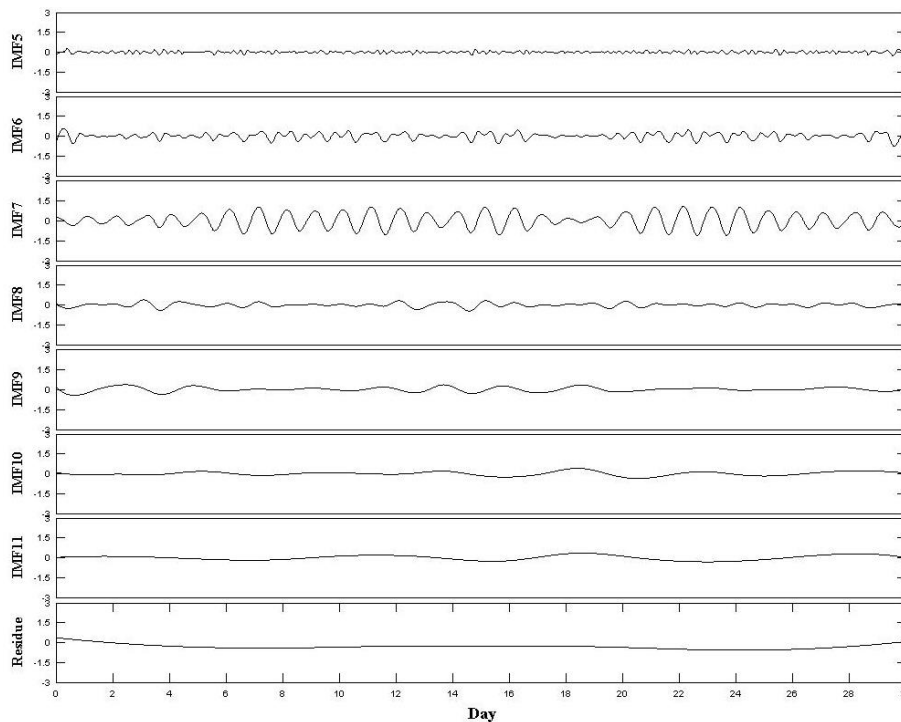


Fig. 7 IMF's of the cable force from EEMD

temperature and those of cable force are depicted in Figs. 6 and 7, respectively. It should be noted that the first four IMF's for both quantities are not included in these figures because they are all high-frequency measurement noises and will be filtered out in the subsequent analysis. Comparison of Figs. 6 and 7 with Figs. 3 and 4 obviously verifies the success of applying EEMD. Furthermore, it is clear from the IMF's in Figs. 6 and 7 together with their corresponding Fourier amplitude spectra plotted in Figs. 8 and 9 that IMF 5 to IMF 8 of the effective temperature and the cable force are all primarily contributed by the frequency components at 1 cycle/day and 2 cycle/day. Accordingly, the combination of IMF 5 up to IMF 8 for the effective temperature is believed to represent the daily temperature variation. On the other hand, the remained IMF 9 up to the residue in Fig. 6 are very likely to indicate the season temperature variation.

#### 4. CORRELATION ANALYSIS FOR EFFECTIVE TEMPERATURE AND CABLE FORCE

After classifying the effective temperature into three parts including the daily variation, the season variation, and the high-frequency noise, the correlation analysis is again conducted between each of the first two major parts and any possible combination for the IMF's of the cable force with the consideration of optimal time shift. With no surprise, the combination of IMF 5 to IMF 8 for the cable force, with similar frequency contents to those for the effective temperature, holds the maximum correlation coefficient of  $-0.98$  under a time shift of 105 minutes. Such a high value of correlation coefficient evidently indicates the almost perfect correlation between the

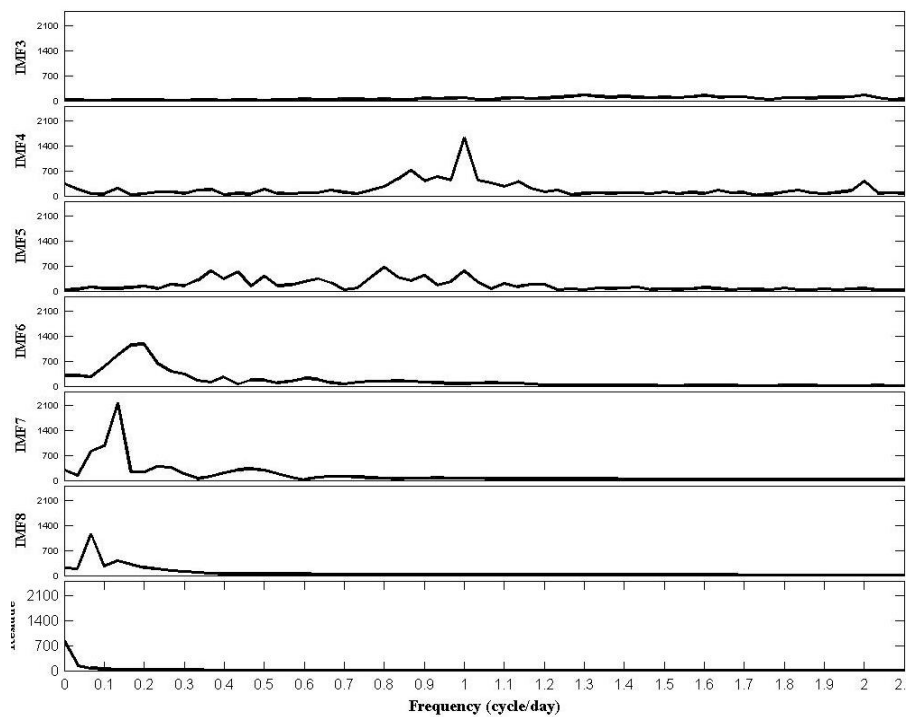


Fig. 8 Fourier Spectra for IMF's of effective temperature

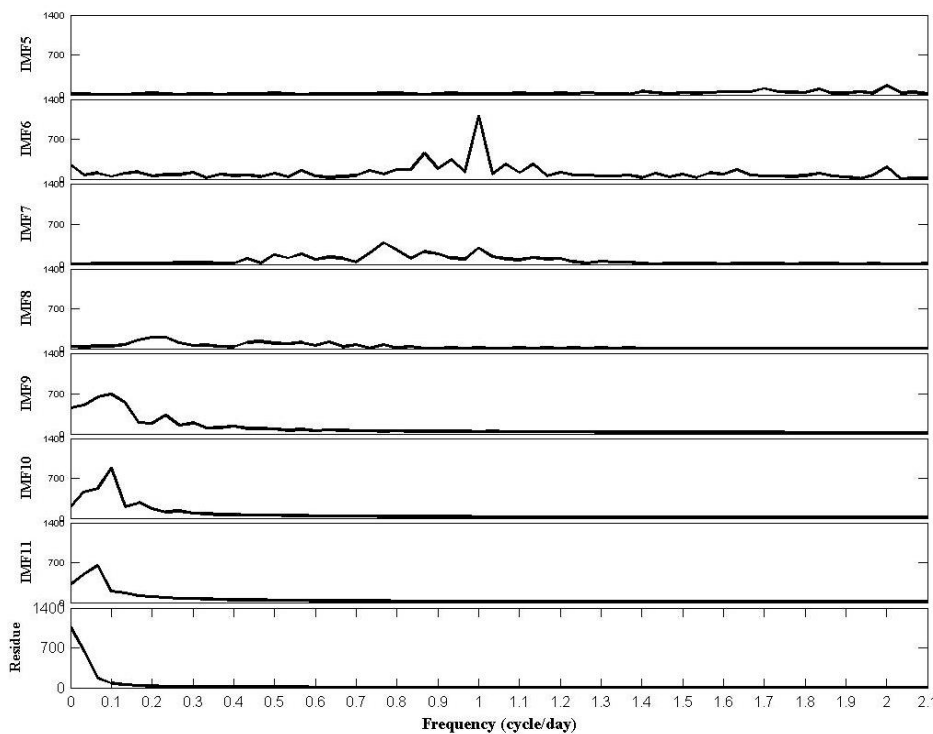


Fig. 9 Fourier Spectra for IMF's of the cable force

daily variations of both quantities. As for the season variation, the combination of IMF 9 up to the residue for the cable force is also found to correlate best with those for the effective temperature at a coefficient of  $-0.90$  under a time shift of 330 minutes. Detailed results for varying different time shifts also reveal that the correlation coefficient is quite sensitive to the time shift in the case of daily variation, but seems to be indifferent with the alternation of time shift in the case of season variation. If both the daily and season components are added together and the corresponding optimal time shifts are also considered, the correlation coefficient between the cable force and the effective temperature becomes  $-0.87$ .

In addition to the one-month data of Cable E13 measured in the winter as previously discussed, the corresponding data for the other three seasons are also taken to perform EEMD decompositions and the subsequent correlation analysis. The same procedures are further applied to analyze the other two cables, Cable E10 and Cable E17. Table 1 summarizes the values of correlation coefficient in different cases together with the associated optimal time shifts listed in the parenthesis. It needs to be mentioned that the positive value of time shift signifies the moving of temperature toward the earlier time instant, while its negative denotes the opposite. All the values of correlation coefficient for different cases of daily variation are no less than  $-0.97$  and their corresponding optimal time shifts range from 0 to 105 minutes. On the other hand, the values of correlation coefficient associated with various cases of season variation are in the interval between  $-0.78$  and  $-0.93$  with a wide time shift range from  $-405$  to

Table 1: Correlation coefficients and optimal time shifts for different seasons of 3 cables

Cable Number	Season	Correlation coefficient (optimal time shift)		
		Daily variation	Season variation	Combination
E10	Spring	$-0.98$ (0 mins)	$-0.83$ ( $-375$ mins)	$-0.94$
	Summer	$-0.97$ (15 mins)	$-0.78$ (240 mins)	$-0.91$
	Autumn	$-0.97$ (15 mins)	$-0.83$ ( $-405$ mins)	$-0.90$
	Winter	$-0.98$ (30 mins)	$-0.87$ (105 mins)	$-0.88$
E13	Spring	$-0.98$ (75 mins)	$-0.90$ ( $-105$ mins)	$-0.93$
	Summer	$-0.97$ (60 mins)	$-0.88$ (360 mins)	$-0.93$
	Autumn	$-0.98$ (90 mins)	$-0.85$ ( $-180$ mins)	$-0.90$
	Winter	$-0.98$ (105 mins)	$-0.90$ (330 mins)	$-0.86$
E17	Spring	$-0.99$ (45 mins)	$-0.92$ ( $-30$ mins)	$-0.94$
	Summer	$-0.99$ (45 mins)	$-0.91$ (345 mins)	$-0.95$
	Autumn	$-0.99$ (60 mins)	$-0.93$ ( $-60$ mins)	$-0.95$
	Winter	$-0.98$ (90 mins)	$-0.93$ (375 mins)	$-0.87$

375 minutes. Since the correlation coefficient is not sensitive to the time shift for the season variation, the wide range of optimal time shifts is not surprising. Even though the values of correlation coefficient for the cases of season variation still indicate a strong correlation, this relationship is certainly not as solid as that demonstrated in the cases of daily variation. The reason for this disparity may come from the length of the investigated time histories is not adequate to fully reflect the variation of the season or long-term effect.

## 5. CONCLUSIONS

The recent works by the authors and the others demonstrate that temperature variation is the dominant environmental factor to induce the variation of stay cable force. An effective temperature defined by the authors to combine all the contributions from stay cable, bridge girder, and pylon was also found to be particularly correlated with the cable force. Using the data collected from an extradosed bridge located in central Taiwan, this work further applies the ensemble empirical mode decomposition to process the time histories of cable force and effective temperature. It is evidently observed that the cable force and effective temperature can both be categorized into daily variation, season variation, and high-frequency noise with the order of decreasing weight. Moreover, the correlation analysis conducted for the decomposed variations of both quantities undoubtedly indicates that the daily and season variations with different time shifts have to be distinguished for accurately evaluating the temperature effect on the variation of cable force. Consistent results for all the four seasons and all the three investigated stay cables confirm the validity and stability of the proposed method, which will serve as a corner stone to define an effective damage index for the health monitoring of cable-stayed bridges.

## REFERENCES

- Chen, C.C., Wu, W.H. and Shih, Y.D. (2010), "Effects of environmental variability on stay cable frequencies", *Proceedings of Second International Symposium on Life-Cycle Civil Engineering*, Taipei, Taiwan.
- Chen, C.C., Wu, W.H. and Liu, C.Y. (2012), "Effects of temperature variation on cable forces of an extradosed bridge", *Proceedings of Sixth European Workshop on Structural Health Monitoring*, Dresden, Germany.
- Chen, C.C., Wu, W.H. and Tseng, H.-Z. (2008), "Measurement of ambient vibration signal of shorter stay cables from stressing to service stages", *Proceedings of Fourth European Workshop on Structural Health Monitoring*, Krakow, Poland.
- Huang, N.E., Shen, Z., Long, S.R., Wu, M.C., Zheng, H.H., Yen, Q., Tung, N.C. and Liu, H.H. (1998), "The empirical mode decomposition and the Hilbert spectrum for nonlinear and nonstationary time series analysis", *Proc. R. Soc. Lond. A*, **454**, 903–993.
- Wu, Z. and Huang, N.E. (2009), "Ensemble empirical mode decomposition: a noise-assisted data analysis method", *Adv. Adapt. Data Anal.*, **1**(1), 1-41.